

Research paper

Robust and adaptive techniques for numerical simulation of nonlinear partial differential equations of fractional order



Kolade M. Owolabi^{a,b}

^a Department of Mathematical Sciences, Federal University of Technology, PMB 704, Akure, Ondo State, Nigeria

^b Institute for Groundwater Studies, Faculty of Natural and Agricultural Sciences, University of the Free State, Bloemfontein 9300, South Africa

ARTICLE INFO

Article history:

Received 15 March 2016

Revised 24 August 2016

Accepted 27 August 2016

Available online 29 August 2016

MSC:

34A34

35A05

35K57

65L05

65M06

93C10

Keywords:

Fourier spectral method

Exponential integrator

Fractional reaction-diffusion

Nonlinear PDEs

Numerical simulations

Spatiotemporal structures

ABSTRACT

In this paper, some nonlinear space-fractional order reaction-diffusion equations (SFORDE) on a finite but large spatial domain $\mathbf{x} \in [0, L]$, $\mathbf{x} = \mathbf{x}(x, y, z)$ and $t \in [0, T]$ are considered. Also in this work, the standard reaction-diffusion system with boundary conditions is generalized by replacing the second-order spatial derivatives with Riemann-Liouville space-fractional derivatives of order α , for $0 < \alpha < 2$. Fourier spectral method is introduced as a better alternative to existing low order schemes for the integration of fractional in space reaction-diffusion problems in conjunction with an adaptive exponential time differencing method, and solve a range of one-, two- and three-components SFORDE numerically to obtain patterns in one- and two-dimensions with a straight forward extension to three spatial dimensions in a sub-diffusive ($0 < \alpha < 1$) and super-diffusive ($1 < \alpha < 2$) scenarios. It is observed that computer simulations of SFORDE give enough evidence that pattern formation in fractional medium at certain parameter value is practically the same as in the standard reaction-diffusion case. With application to models in biology and physics, different spatiotemporal dynamics are observed and displayed.

© 2016 Elsevier B.V. All rights reserved.

1. Introduction

The subject of fractional calculus is as old as classical calculus, which is based on a generalization of integration and ordinary differentiation of arbitrary non-integer order. The idea of fractional derivative has been an active subject of interest over the years, not only among the mathematicians but also among the engineers and physicists [50,55]. Fractional diffusion equations have been considered useful due to their application in some areas of science, such as biology, chemistry, ecology, physics, mechanics and engineering. A considerable number of important physical problems in these subject areas are modelled mathematically in the form of fractional differential equations (FDE). The FDE models are proved to be more adequate [50] and rich in pattern formation processes [9] than the classical or integer order models. The second order spatial derivative in standard time-dependent reaction-diffusion equation is replaced by a fractional (non-integer order of less than two, that is $0 < \alpha < 2$) derivative in a fractional reaction-diffusion equation. The fractional reaction-diffusion problems are largely found combining the fractional diffusion term with a standard reaction term.

E-mail address: mkowolax@yahoo.com, kmowolabi@futa.edu.ng

<http://dx.doi.org/10.1016/j.cnsns.2016.08.021>

1007-5704/© 2016 Elsevier B.V. All rights reserved.

In recent times, fractional differential equations are considered as an important tool suitable to describe and model various physical phenomena such as pattern formation, Turing structures, spatio-temporal chaos and nonlinear waves (solitons or spiral waves) [15,22]. In development, the generalized calculus has been hampered consistently due to the fact that many fractional derivative problems have no exact solutions unlike the classical case. Inspired and motivated with the trend of ongoing research in this area, authors [62,63] have applied Homotopy analysis method to obtain analytical solutions of fractional reaction-diffusion equations for both initial and boundary value problems. Mohyud-Din and Noor [35] proposed the variation iteration method by using He's polynomial to solve higher-order nonlinear boundary value problems. Momani and Odibat [36], Odibat and Momani [39] also applied variation iteration method to solve various nonlinear differential equations of fractional order. Chen [12] studied fractional diffusion equations by applying the Kansa method, in which the MultiQuadratics and thin plate spline serve as the radial basis function. Momani et al. [37] considered the generalized transform method for solving space-time fractional diffusion-wave problem. A multistep differential transform approach was introduced by Odibat and Momani [41] to address both chaotic and non-chaotic systems. Ray [52] considered a two-step Adomian decomposition method for the analytic solution of space fractional diffusion equation. Similarly, Yu et al. [64] applied the Adomian decomposition technique to solve linear and nonlinear space fractional reaction-diffusion equations. Comparison between the Adomian decomposition method and differential transform technique when applied to solve nonlinear initial value problems was reported by Hassan [21]. Other notable techniques such as the Taylor and matrix methods which have been applied to solve various fractional equations are well classified in [17,40,51] and references therein.

The efficient and accurate simulation of such class of reaction-diffusion systems, is challenging especially in higher dimensions. The reason is not far fetch from the fact that such system combines stiff diffusion term with nonlinear reaction term. When such is discretized, it results to a stiff nonlinear systems of ordinary differential equations (ODEs). A standard technique for solving fractional-reaction-diffusion equation is to apply a finite volume, finite element or finite difference discretization of the fractional derivative operator, and then formulate a lower-order scheme such as semi-implicit Euler for the time evolution of the solution. Unfortunately, in higher space dimensions, numerical simulations based upon the more conventional ideas such as finite difference, element and volume methods become more time consuming, as simulations in two or higher dimensions require an hour or more runtime.

The primary interest in the present work is not really in one dimensional simulations, but to formulate a well-versatile, reliable, efficient and adaptive methods that will be suitable to address any points and queries that may naturally arise with the simulation of fractional reaction-diffusion systems in higher dimensions. Hence, Fourier spectral method is introduced as a reliable alternative approach to the known lower-order discretization methods for solving space fractional reaction-diffusion equations. The main merit of this technique is that it permits a full diagonal representation of the fractional derivative operator, with ability to gain spectral convergence irrespective of the fractional power in the system of equation. Another advantage is that spectral methods can be used to remove the stiffness issue often associated with the fractional reaction-diffusion problems, and thereby permit the use of bigger time-steps with any explicit time stepping solver. This further enhances the code to run very fast on standard PC or Laptop.

The aims of this paper are in folds. In [Section 2](#), further useful preliminaries of fractional reaction-diffusion equations are presented. In [Section 3](#), some adaptive numerical techniques for the solution of fractional reaction-diffusion problems are formulated. In [Section 4](#), numerical simulations for a range of existing problems in one-, two- and three-components that are of practical interest are introduced and carried out, these problems are largely encountered in the application areas of biology, physics, chemistry and engineering which are formulated in the form of fractional-in-space reaction-diffusion equations. The work is finally concluded with [Section 5](#).

2. Fractional order derivatives and fractional fourier transform

This section begins with the basic properties and some of the advantages of using the Riemann-Liouville fractional calculus [10,27,50,51].

Definition 2.1. For $\alpha \in (-\infty, \infty)$, the Riemann-Liouville fractional integral is given as follows: If $f(\mathbf{x}) \in ([a, b])$ and $a < \mathbf{x} < b$, then

$$I_{\alpha+}^{\alpha} f(\mathbf{x}) = \frac{1}{\Gamma(\alpha)} \int_a^{\mathbf{x}} \frac{f(t)}{(\mathbf{x} - t)^{1-\alpha}} dt. \quad (1)$$

Definition 2.2. For $\alpha \in (0, \infty)$,

$$D_{\alpha+}^{\alpha} f(\mathbf{x}) = \frac{1}{\Gamma(1-\alpha)} \frac{d}{d\mathbf{x}} \int_a^{\mathbf{x}} \frac{f(t)}{(\mathbf{x} - t)^{\alpha}} dt \quad (2)$$

is known as the Riemann-Liouville fractional derivative of order α [50,55].

One of the major advantages of using the Riemann-Liouville fractional derivative within the variation principles is due to the possibility of defining the integration by parts as the fractional reaction-diffusion problems becomes the classical case whenever α becomes an integer [5,54]. Additionally, it satisfies virtually all the mathematical principle under the scope of fractional calculus, especially when using Laplace transform we obtain initial condition with fractional power index (exponent) which is actually realistic in practical and mathematical point of views because we are in the scope of fractional

calculus. As a result, most researchers [4,57] applauded the use of the Riemann-Liouville definition due to its suitability and adaptability. Readers are referred to classical books and research papers [10,27,30,33,34,38,42,50,53,65–68] for details underlying theory as well as comprehensive review of the fractional differential equations.

A general nonlinear initial-boundary value space fractional reaction-diffusion equation can be written as

$$\partial_t \mathbf{u}(\mathbf{x}, t) = \delta \Delta^\alpha \mathbf{u}(\mathbf{x}, t) + \mathcal{F}(\mathbf{u}(\mathbf{x}, t)), \quad 0 < \alpha \leq 2, \quad (3)$$

subject to initial condition

$$\mathbf{u}(\mathbf{x}, 0) = f(\mathbf{x}) \quad (4)$$

where $\mathbf{u} = (u, v, w)$ represents the species concentration or population density. δ is the diffusion tensor or conductivity, $\mathbf{u} = (x, y, z)^T$, is the position vector in the directions x , y and z , $\alpha > 0$ is the fractional power, \mathcal{F} is the nonlinear reaction term. The term $\Delta^\alpha = \left(\frac{\partial^\alpha}{\partial x^\alpha}, \frac{\partial^\alpha}{\partial y^\alpha}, \frac{\partial^\alpha}{\partial z^\alpha} \right)^T$, T -transpose, denotes the Riemann-Liouville fractional gradient or simply fractional Laplacian operator, with

$$\begin{aligned} \frac{\partial^\alpha}{\partial x^\alpha} u(x, y, z) &= \frac{1}{\Gamma(1-\alpha)} \frac{\partial}{\partial x} \int_0^x \frac{u(s, y, z)}{(x-s)^\alpha} ds, \\ \frac{\partial^\alpha}{\partial y^\alpha} u(x, y, z) &= \frac{1}{\Gamma(1-\alpha)} \frac{\partial}{\partial y} \int_0^y \frac{u(s, x, z)}{(y-s)^\alpha} ds, \\ \frac{\partial^\alpha}{\partial z^\alpha} u(x, y, z) &= \frac{1}{\Gamma(1-\alpha)} \frac{\partial}{\partial z} \int_0^z \frac{u(s, x, y)}{(z-s)^\alpha} ds. \end{aligned}$$

Solutions to (3) exhibit accelerating fronts with power-law leading edges, with behaviour encountered in many ecological invasive species models [3,49]. Equation (3) is regarded as a special type of the one-dimensional reaction-diffusion equation

$$\partial_t u = [Lu(\cdot, t)](\mathbf{x}) + \mathcal{F}(\mathbf{u}(\mathbf{x}, t)), \quad u(\mathbf{x}, 0) = u_0(\mathbf{x}), \quad \mathbf{x} \in \mathbb{R}^d, \quad (5)$$

where L is a pseudo-differential operator (see for instance [44,45,47],) and $f : \mathbb{R}^d \times \mathbb{R} \rightarrow \mathbb{R}$. Also in this section, it is important we outline some of the useful basic definitions and lemmas as earlier introduced in [10,50,51].

Next, we need to familiarize with the definitions of the continuous and discrete fractional Fourier transforms.

Definition 2.3. For a function $u \in S(\mathbb{R})$ (Schwartzian space), $S(\mathbb{R})$ being the space of rapidly decreasing test functions on the real axis \mathbb{R} , the Fourier transform \hat{u} is defined as

$$\hat{u}(\omega) = (\mathcal{F}u)(\omega) = \int_{-\infty}^{\infty} u(t) e^{i\omega t} dt, \quad \omega \in \mathbb{R}. \quad (6)$$

The inverse Fourier transform is given in the form

$$u(t) = (\mathcal{F}^{-1}\hat{u})(t) = \frac{1}{2\pi} \int_{-\infty}^{\infty} \hat{u}(\omega) e^{-i\omega t} d\omega, \quad t \in \mathbb{R}. \quad (7)$$

In what follows, we enumerate some properties of the fractional Fourier transform.

(i) Let $V(\mathbb{R})$ be the set of functions such that

$$V(\mathbb{R}) = \left\{ v \in S(\mathbb{R}) : \left. \frac{d^n v}{d\mathbf{x}^n} \right|_{\mathbf{x}=0} = 0, \quad n = 0, 1, 2, \dots \right\}. \quad (8)$$

The Lizorkin space $\Phi(\mathbb{R})$ is defined as the Fourier pre-image of the space $V(\mathbb{R})$ in the space $S(\mathbb{R})$, i.e.,

$$\Phi(\mathbb{R}) = \{ \varphi \in S(\mathbb{R}) : \hat{\varphi} \in V(\mathbb{R}) \}. \quad (9)$$

In other words, a function $\varphi \in \Phi(\mathbb{R})$ if the orthogonality condition

$$\int_{-\infty}^{+\infty} g^n \varphi(\wp) d\wp = 0, \quad n = 0, 1, 2, \dots \quad (10)$$

is satisfied.

This operator was shown to remain invariant with respect to fractional integration and differentiation. This feature gives credit to the Lizorkin space to be a useful and versatile working tool with Fourier transform, fractional integration and differentiation operators. For further identities and details of the Lizorkin space, readers are referred to the classical book and research paper in [55,56] and the references therein.

(ii) For a function $u \in \Phi(\mathbb{R})$, the fractional Fourier transform of the order $\alpha > 0$, \hat{u}_α , is defined as

$$\hat{u}_\alpha(\omega) = (\mathcal{F}_\alpha u)(\omega) = \int_{-\infty}^{+\infty} e^{i\text{sign}(\omega)|\omega|^{\frac{1}{\alpha}} t} u(t) dt, \quad \omega \in \mathbb{R}, \quad (11)$$

and the inverse fractional Fourier transform of order $\alpha > 0$ is given by

$$(\mathcal{F}_\alpha^{-1} u)(\omega) = \frac{1}{2\pi\alpha} \int_{-\infty}^{+\infty} e^{-i\text{sign}(\omega)|\omega|^{\frac{1}{\alpha}}t} \hat{u}_\alpha(\omega) \omega^{\frac{1-\alpha}{\alpha}} d\omega, \quad t \in \mathbb{R}. \quad (12)$$

Hence we have,

$$\mathcal{F}_\alpha^{-1} \mathcal{F}_\alpha u = u. \quad (13)$$

One can see clearly that for $\alpha = 1$, the fractional Fourier transform \mathcal{F}_α is reduced to the conventional Fourier transform \mathcal{F} . These transforms are connected by the relation

$$\hat{u}_\alpha(\omega) = (\mathcal{F}_\alpha u)(\omega) = (\mathcal{F}u)(\mathbf{x}) = \hat{u}(\mathbf{x}), \quad \mathbf{x} = \text{sign}(\omega)|\omega|^{\frac{1}{\alpha}}. \quad (14)$$

3. Numerical techniques for fractional reaction-diffusion

In this section, we briefly discuss the application of the Fourier Spectral method used for the spatial discretization of problem of the form (3).

3.1. Fourier spectral method for space fractional reaction-diffusion

Spectral methods are approximation techniques for the computation of the solutions to ordinary and partial differential equations. They are based on a polynomial expansion of the solution. Despite the facts that spectral methods gain tremendous higher order convergence when compared to low order stencils and being in nature nonlocal, only a few handful works has been reported of spectral methods for the solution of space fractional reaction-diffusion equations. A spectral technique for the weak solution of the space-time fractional diffusion equation was considered by Li and Xu [28,29]. Also, Hanert [19] considers the use of a Chebyshev spectral element approach for the numerical solution of the fractional Riemann-Liouville advection-diffusion equation for tracer transport. Khader [25] introduces the use of a Chebyshev Galerkin method to spatially discretize space fractional diffusion equation in the Caputo sense. However, most previous works done were restricted to only one-dimensional experiments, which are easily undertaken. Knowing well that the nature of problem of the type (3) allows the use of two classical methods, one in space and the other in time. As a result, we introduce Fourier spectral method to discretize in space, and advance the resulting system of ordinary differential equations with the modified version of the exponential time-differencing schemes [13,24]. To present this approach, we first write the fractional reaction-diffusion equation (3) in the general form

$$\left. \begin{aligned} \frac{\partial u(\mathbf{x}, t)}{\partial t} &= \delta(\Delta)^\alpha u(\mathbf{x}, t) + \mathcal{F}(u, t), \quad 0 < \alpha \leq 2, \\ u(\mathbf{x}, 0) &= u_0(\mathbf{x}) \end{aligned} \right\} \quad (15)$$

where $u(x, t)$ is the species density in one $\mathbf{x} = (x)$, two $\mathbf{x} = (x, y)^T$ or three $\mathbf{x} = (x, y, z)^T$ dimensions, $\delta = (\delta_i)$, $i = 1, 2, 3 \in \mathbb{R}_+$ are their constant matrices which describe the respective diffusion coefficients. The operator $(\Delta)^\alpha$ remains the fractional Laplacian operator associated with the species, and the term $\mathcal{F}(u, t)$ represents the biological or chemical reactions.

Though there are several existing numerical methods that can be used to discretize (15) in space. It should be noted that the fractional differential operator is non-local red operator, which often results to a serious computational and numerical challenges that are rarely encountered in the context of classical second-order reaction-diffusion equations. In addition, for the space-fractional diffusion equations, most numerical techniques often result in relatively sparse matrices with complicated structures [61]. In this research paper, we employ fractional Fourier spectral methods [23,26] to discretize the space-fractional derivatives.

Next, we apply the fractional Fourier transform operator \mathcal{F}_α (11) on both sides of (15), making use of Kilbas et al. [26] property

$$(\mathcal{F}_\alpha D_\beta^\alpha u)(\omega) = (-ic_\alpha(\beta)\omega)(\mathcal{F}_\alpha u)(\omega), \quad (\alpha > 0; \beta, \omega \in \mathbb{R}) \quad (16)$$

where c_α a constant is defined as

$$c_\alpha = \sin(\alpha\pi/2) + i\text{sign}(\omega)(1 - 2\beta)\cos(\alpha\pi/2),$$

we obtain the ODEs system

$$\left. \begin{aligned} \frac{\partial \hat{u}_\alpha}{\partial t}(\omega, t) &= \delta(ic_\alpha(\beta)\omega)\hat{u}_\alpha(\omega, t) + \widehat{\mathcal{F}_\alpha(u, t)}, \quad 0 < \alpha \leq 2, \\ \hat{u}_\alpha(\omega, 0) &= \hat{u}_{\alpha,0}(\omega) \end{aligned} \right\} \quad (17)$$

where c_α is a constant defined as

$$c_\alpha = \sin(\alpha\pi/2) + i\text{sign}(\omega)(1 - 2\beta)\cos(\alpha\pi/2). \quad (18)$$

This approach yields a full diagonal representation of the fractional operator and provides a better spectral convergence regardless of the fractional power in the given problem.

Application to higher spatial dimensions is practically the same as illustrated to one- and two-dimensional problem above. Careful attention should be given in order to filter the occurrence high frequencies appropriately, since the nonlinear term is evaluated in physical space and then transformed to Fourier space. This can lead to problems with aliasing [24,46].

The essential point is that once the stiffness issue is removed one can employ any explicit higher-order time integrators [1,8,24,31,46,59,60] to rapidly and accurately advance forwards in time, this is vastly superior to the use of implicit schemes most especially in higher dimensions. Hence, for the temporal discretization we engage an improved fourth-order exponential time differencing Runge-Kutta (ETDRK4) scheme as proposed by Cox and Matthews [13], which was later modified by Kassam and Trefethen [24]

$$\begin{aligned} a_n &= e^{\mathbf{L}h/2} u_n + \mathbf{L}^{-1}(e^{\mathbf{L}h/2} - \mathbf{I})\mathbf{F}(u_n, t_n), \\ b_n &= e^{\mathbf{L}h/2} u_n + \mathbf{L}^{-1}(e^{\mathbf{L}h/2} - \mathbf{I})\mathbf{F}(a_n, t_n + h/2), \\ c_n &= e^{\mathbf{L}h/2} u_n + \mathbf{L}^{-1}(e^{\mathbf{L}h/2} - \mathbf{I})[2\mathbf{F}(b_n, t_n + h/2) - \mathbf{F}(u_n, t_n)], \\ u_{n+1} &= e^{\mathbf{L}h} u_n + h^{-2} \mathbf{L}^{-3} \{[-4\mathbf{I} - h\mathbf{L} + e^{\mathbf{L}h}(4\mathbf{I} - 3h\mathbf{L} + (h\mathbf{L})^2)]\mathbf{F}(u_n, t_n) \\ &\quad + 2[2\mathbf{I} + h\mathbf{L} + e^{\mathbf{L}h}(-2\mathbf{I} + h\mathbf{L})](\mathbf{F}(a_n, t_n + h/2) + \mathbf{F}(b_n, t_n + h/2)) \\ &\quad + [-4\mathbf{I} - 3h\mathbf{L} - (h\mathbf{L})^2 + e^{\mathbf{L}h}(4\mathbf{I} - h\mathbf{L})]\mathbf{F}(c_n, t_n + h)\}. \end{aligned} \quad (19)$$

To save time and avoid repetition, information on derivation, stability and convergence of the ETDRK4 and other explicit exponential integrators can be found in [13,14,24,44,46,47].

4. Numerical experiments

In this section, we choose and introduce a range of illustrative examples that are still of current and recurring interest in physics, chemistry and biology, which also cover pitfalls and natural questions that may naturally arise.

4.1. One-component example

Complex cubic-quintic Ginzburg-Landau equation: The complex cubic-quintic Ginzburg-Landau equation (CCQGLE) has been regarded as one of the most dissipative systems that has been intensively studied for describing weakly nonlinear phenomena [45]. The fractional CCQGLE is given in the form

$$\partial_t U = \vartheta U + (\beta_1 + i\gamma_1) \Delta^\alpha U - (\beta_3 - i\gamma_3) |U|^2 U - (\beta_5 - i\gamma_5) |U|^4 U, \quad (20)$$

where U is the species concentration or population densities, ϑ represents the linear loss, β_1 defines the angular spectral filtering, β_3 stands for the nonlinear loss or gain, and β_5 is the saturation of the nonlinear loss or gain. The γ_i , $i = 1, 3, 5$ symbolize the diffraction coefficient, self focusing and saturation of the nonlinear refractive index respectively.

Attempts have been made to explore the exact periodic and solitary wave solutions of nonlinear reaction-diffusion equation of the form (20) involving cubic-quintic nonlinearity along with time-dependent convection coefficients. Effect of varying model coefficients on the physical parameters of solitary wave solutions is demonstrated in [7]. Depending upon the choice parametric condition, the periodic, double-kink, bell and anti-kink-type solutions for cubic-quintic nonlinear classical reaction-diffusion equation have been reported. Such solutions can be used to explain various biological and physical phenomena. Review of some of the basic properties of the equation are well discussed in [6], as well as applications to a number of nonlinear waves phenomena.

The major element in the long time dynamics of pattern forming systems is a class of solutions called coherent structures or solitons [45], which could be a profile of light intensity, magnetic field or temperature [11]. Other observed phenomena include the superconductivity, superfluidity, Bose-Einstein condensation [58], liquid crystals and string theory, nonlinear waves and phase transitions [2].

In one dimension, we simulate (20) subject to a periodic boundary condition and random the initial data ($\text{rand}(N)*\rho_1$), where ρ_1 is a small noise of orders in the interval $[0.01, 0.1]$, and N is the number of interior points defined on the interval

$$\{x_1 = l_1, \dots, x_i = a + (i - 1)\Delta x, \dots, x_N = l_2\}, \quad \text{for } \Delta x = \frac{|l_2 - l_1|}{N - 1}. \quad (21)$$

The simulation results in Fig. 1(a-c) show the effects of fractional power α at instances of $\alpha = 0.5$, $\alpha = 1.0$ and $\alpha = 1.5$ which corresponds to the sub-diffusive, diffusive and super-diffusive scenarios. Panel (a) corresponds to the solution obtained at different instances of fractional power α at $t = 30$, see the figure caption for other parameter values.

A vast variety of nonlinear oscillatory traveling waves phenomena are obtained in panels (a-d) of Fig. 1. In (a), the waves pattern are propagating from the origin are unstable but becoming stable towards the empty space. The waves in panels (b), (c) and (d) are the surface plots obtained at $\alpha = 0.5$, $\alpha = 1.1$ and $\alpha = 1.85$ which correspond to the sub-diffusive and super-diffusive scenarios respectively. It should be noted that we can obtain a vast variety of nonlinear dynamic which often lead to either stationary soliton or oscillatory structures whenever a stable equilibrium solution which usually changes spontaneously with the choice of physical parameter to stationary dissipative structures by Turing instability or limit cycle by Hopf instability.

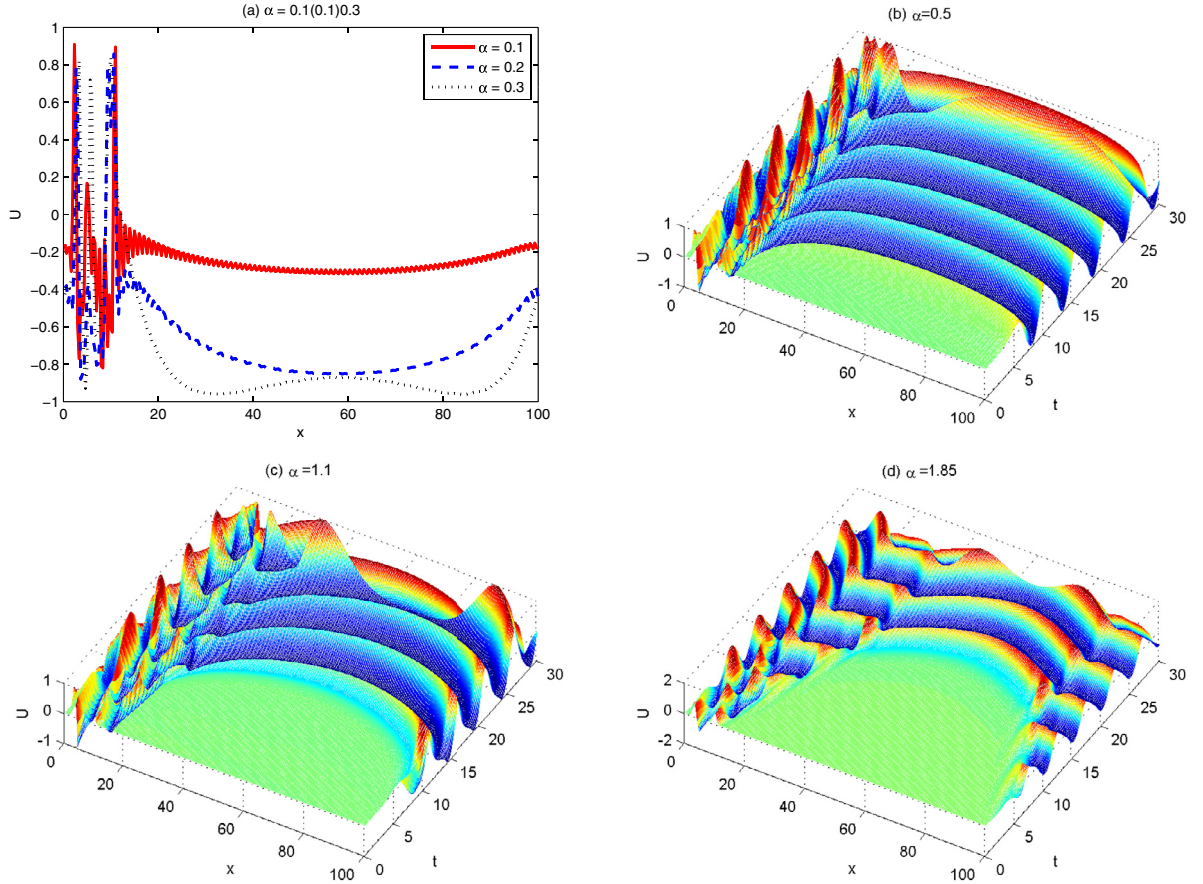


Fig. 1. Numerical results of the fractional CCQGLE equation (20) at $t = 30$. The effects of fractional power α is shown at instances of (a) $\alpha = 0.5$, (b) $\alpha = 1.1$ and (c) at $\alpha = 1.85$. Other parameters values are; $\rho_1 = 0.1$, $\vartheta = 0.04$, $\beta_1 = 0.02$, $\gamma_1 = 0.5$, $\beta_3 = 0.37$, $\gamma_3 = 1.00$, $\beta_5 = 0.03$ and $\gamma_5 = 0.101$. Simulation runs for $N = 100$.

Table 1

The relative error and computational time results for solving equation (20) in one-dimensional space for various values of discretization computed at $t = 1$, $\Upsilon = 35$ and $\alpha = 1.65$. Other parameters are given in Fig. 1.

Method	$N = 16$	$N = 32$	$N = 64$	$N = 128$	$N = 256$	$N = 512$
Finite difference	2.35e-04 0.32s	2.01e-04 0.34s	1.55e-04 0.72s	1.02e-04s 1.12s	0.65e-04 3.33s	7.28e-05 9.06s
Predictor-corrector	3.18e-04 0.41s	5.62e-05 0.33s	2.55e-05 0.36s	1.28e-05 1.77s	6.66e-06 2.45s	2.43e-06 3.11s
Fourier spectral	1.05e-08 0.18s	8.23e-09 0.16s	3.46e-09 0.44s	9.03e-10 0.95s	5.51e-10 1.02s	8.24e-11 2.13s

Table 1 illustrates the performance of the schemes, we compute the relative error defined as

$$\text{relative error} = \frac{\max |\bar{U}_j - U_j|}{\max |\bar{U}_j|}, \quad (22)$$

where \bar{U}_j and U_j is a gold-standard run computed with the schemes [44,47,48] at $\Delta t = 1/2048$ and U_j is numerical values of U at point j . The smooth initial condition is given in the form of a Gaussian pulses

$$U(x, 0) = e^{-20((x-\Upsilon/3)^2)/\Upsilon} - e^{-20((x-\Upsilon/2)^2)/\Upsilon} + e^{-20((x-\Upsilon)^2)/\Upsilon}. \quad (23)$$

The result obtained in **Table 1** provides a strong case for abandoning both the finite difference scheme [32] and predictor-corrector method [43] in favour of Fourier spectral method in conjunction with the ETDRK4. Execution times are also reported in **Table 1** for comparison of the schemes. Obviously, one could give credit to the Fourier spectral method, especially

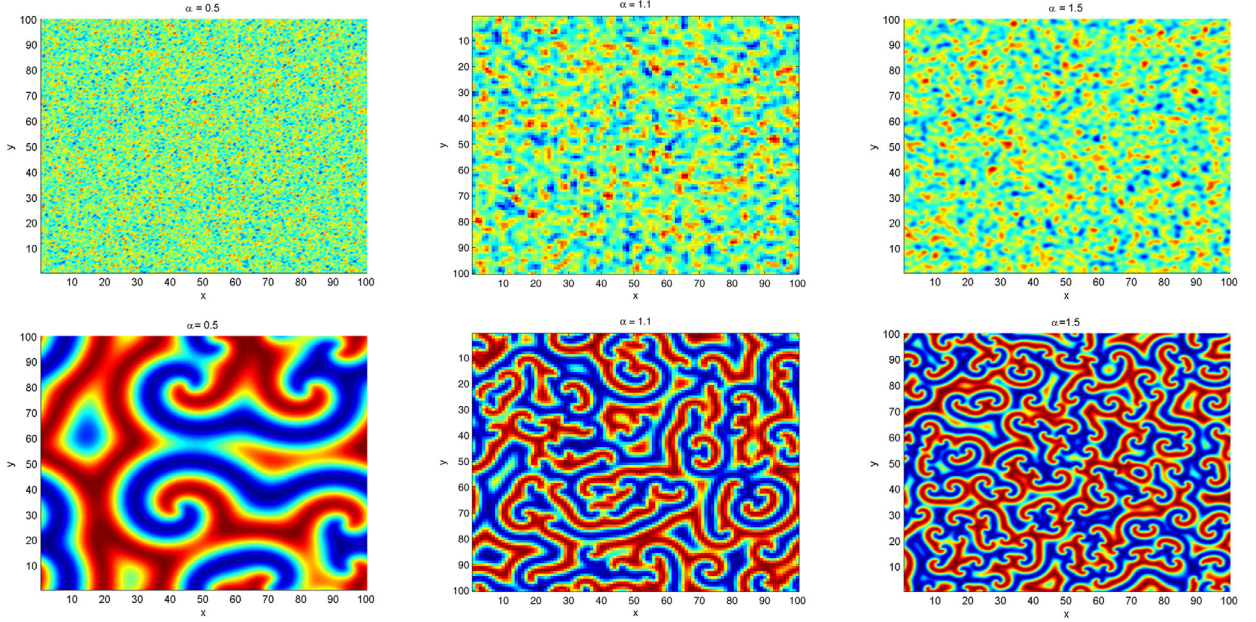


Fig. 2. Simulations in 2D for the fractional CCQGLE Eq. (20) at final time $t = 1$ and $t = 150$ for upper and lower rows respectively. The effects of fractional power α is shown at instances of $\alpha = 0.5$, $\alpha = 1.1$ and $\alpha = 1.5$. Simulation runs for $N = 200$. Other parameters are given in (26).

for larger N . In 2D, simulation with both finite difference and predictor-corrector schemes take between 2 and 4 h to run, compare to Fourier spectral method that requires less than a minute to perform the same task. Hence, we carried out the remaining experiments with the Fourier spectral method.

By following the discussions in Section 3, the Fourier transform of (20) in 2D becomes

$$\hat{U}_t = [\vartheta - (\beta_1 + i\gamma_1)(k_x^2 + k_y^2)]\hat{U} - (\beta_3 + i\gamma_3)|\hat{U}|^2\hat{U} - (\beta_5 + i\gamma_5)|\hat{U}|^4\hat{U},$$

which on rearranging results to ODE of the form

$$\hat{U}_t = \underbrace{\varrho(k_x, k_y)\hat{U}}_{\text{linear}} + \underbrace{\sigma|\hat{U}|^2\hat{U} + \varsigma|\hat{U}|^4\hat{U}}_{\text{nonlinear}} \quad (24)$$

in the Fourier space, with $\varrho(k_x, k_y) = \vartheta - (\beta_1 + i\gamma_1)(k_x^2 + k_y^2)$, $\sigma = -(\beta_3 + i\gamma_3)$ and $\varsigma = -(\beta_5 + i\gamma_5)$. As earlier mentioned, we can split Eq. (24) into linear part which contains the diffusive term, and nonlinear part which harbours the chemical or biological reactions.

In the spirits of [45–48], we adopt the standard discretization technique on a rectangular spatial domain of size $[l_1/2, l_2/2] \times [l_1/2, l_2/2]$, for $l_1 = 0, l_2 = 200$, $n \times n$ uniformly spaced grid points $\mathbf{x}_{ij} = (x_i, y_j)$ with $\Delta x = \Delta y = l/n$ for n even number. With $U(\mathbf{x}_{ij}) = U_{ij}$, $i, j = 1, 2, 3, \dots, n$, we present the Discrete Fourier transform (DFT) of U in 2D as

$$\hat{U}_{k_x k_y} = \Delta x \Delta y \sum_{i=1}^n \sum_{j=1}^n e^{-i(k_x x_i + k_y y_j)} U_{ij}, \quad k_x, k_y = -\frac{n}{2} + 1, \dots, \frac{n}{2}$$

with corresponding DFT in 2D as

$$U_{ij} = \frac{1}{(2\pi)^2} \sum_{k_x=-n/2+1}^{n/2} \sum_{k_y=-n/2+1}^{n/2} e^{i(k_x x_i + k_y y_j)} \hat{U}_{k_x k_y}, \quad i, j = 1, 2, 3, \dots, n$$

where the spatial indexes i and j as well as the wavenumbers k_x and k_y are strictly integers.

We numerically solve (20) in 2D subject to smooth

$$\begin{aligned} U(x, y, 0) = & e^{-20((x-\Upsilon/3)^2 + (y-\Upsilon/3)^2)/\Upsilon} \\ & - e^{-20((x-\Upsilon/2)^2 + (y-\Upsilon/2)^2)/\Upsilon} \\ & + e^{-20((x-\Upsilon/2)^2 + (y-\Upsilon/3)^2)/\Upsilon}. \end{aligned} \quad (25)$$

and random initial conditions computed as $(\text{rand}(N, N)*\rho)$. Parameter values are fixed as;

$$\Upsilon = 40, \rho_1 = 0.1, \vartheta = 0.04, \beta_1 = 0.101, \gamma_1 = 0.5, \beta_3 = 0.37, \gamma_3 = 1.00, \beta_5 = 0.04, \gamma_5 = 0.08. \quad (26)$$

the results are displayed in Fig. 2 at some different instants of fractional power α .

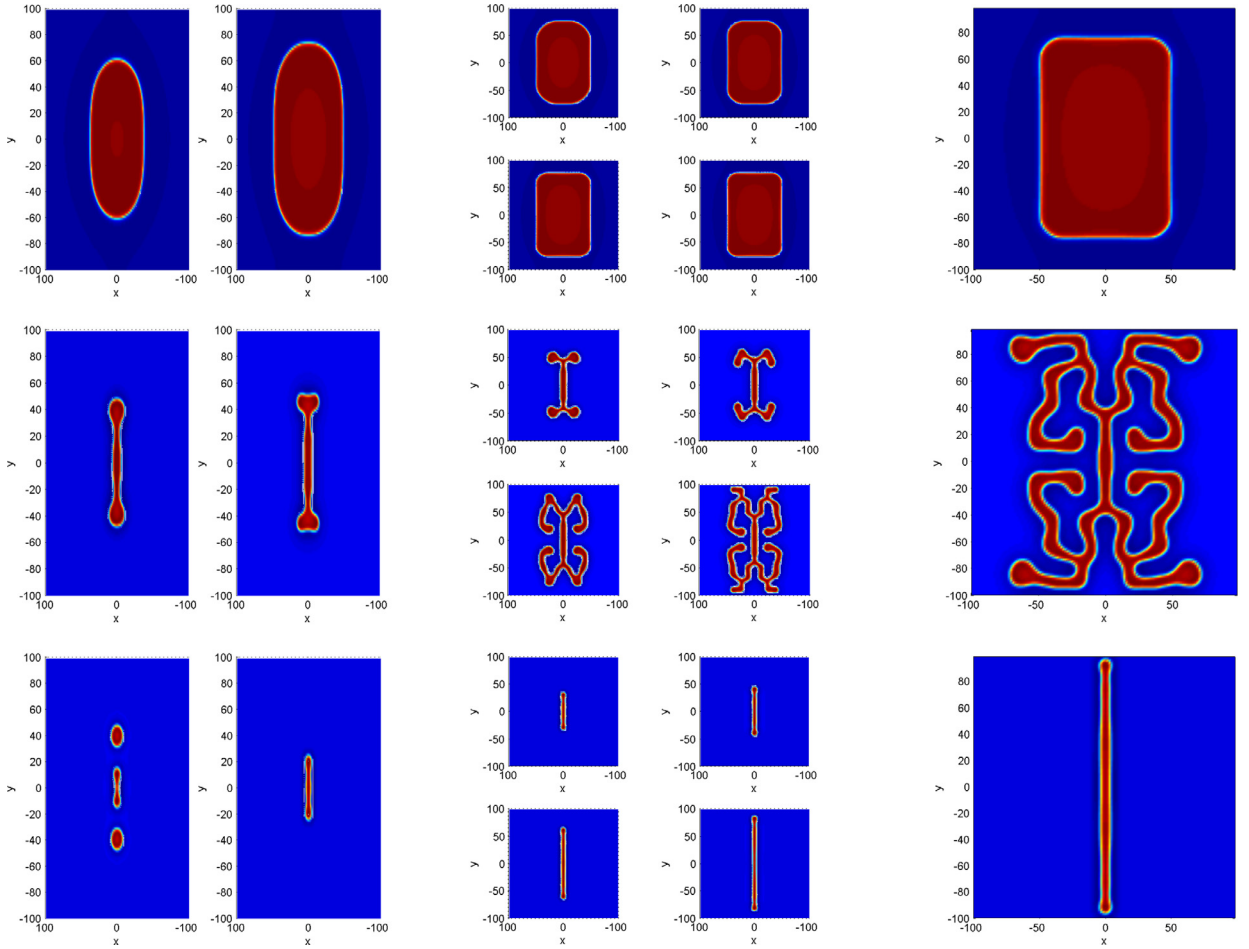


Fig. 3. Simulations in 2D for the fractional activator-inhibitor system (27) at different instants of fractional power α . The upper-, middle- and lower-rows correspond to when $\alpha = 0.5, 1.0, 1.5$, respectively. The columns one, two and three represent numerical results obtained at final time $t = [100, 200]$, $t = [300, 400, 600, 800]$ and $t = 1000$ respectively. Simulation runs for $N = 128$.

4.2. Two-components example

Activator-inhibitor system: In this section, we give extension to our study from a scalar form of fractional reaction-diffusion to a two-components fractional in space called the activator-inhibitor system widely regarded as one of the most interesting and striking group of patterns that arise in models of catalytic reactions. In two components, we present the space fractional reaction-diffusion system

$$\left. \begin{array}{l} \partial_t U = \Delta^\alpha U + U - U^3 - V, \\ \partial_t V = \epsilon \Delta^\alpha V + \delta(U - a_1 V - a_0) \end{array} \right\} \quad (27)$$

where $U = U(\mathbf{x}, t)$ and $V = V(\mathbf{x}, t)$, $\mathbf{x} = \mathbf{x}(x, y) \in \mathbb{R}^2$ are the respective concentrations of chemical species U known as the activator or catalyst and V called the inhibitor, Δ^α remains the fractional Laplacian operator of order α . The activator is known to stimulate its own production and that of the inhibitor through autocatalysis. In turn, the inhibitor slows down the production rate of the activator. The choice of parameters a_0, a_1, δ and ϵ cause one to move from one regime to another, see [18] for details.

In Fig. 3, we simulate with the initial conditions

$$\left. \begin{array}{l} U(x, y, 0) = a_1 V^* + a_0 - 4a_1 V^* e^{-0.1(x^2+0.01y^2)}, \\ V(x, y, 0) = V^* - 2V^* e^{-0.1(x^2+0.01y^2)} \end{array} \right\} \quad (28)$$

carefully chosen to induce nontrivial stationary state and to reveal the sensitivity of some chaotic structures in the activator-inhibitor system. The value of $V^* = (U^* - a_0)/a_1$ is determined from U^* , regarded as the smallest root of the cubic equation $a_1 U^3 + U(1 - a_1) - a_0 = 0$. The state (U, V) is stable. Here, the computational experiment utilizes 128×128 Fourier nodes on a 200×200 grid. In the experiment, different types of dynamics are observed and we also realized that the distributions

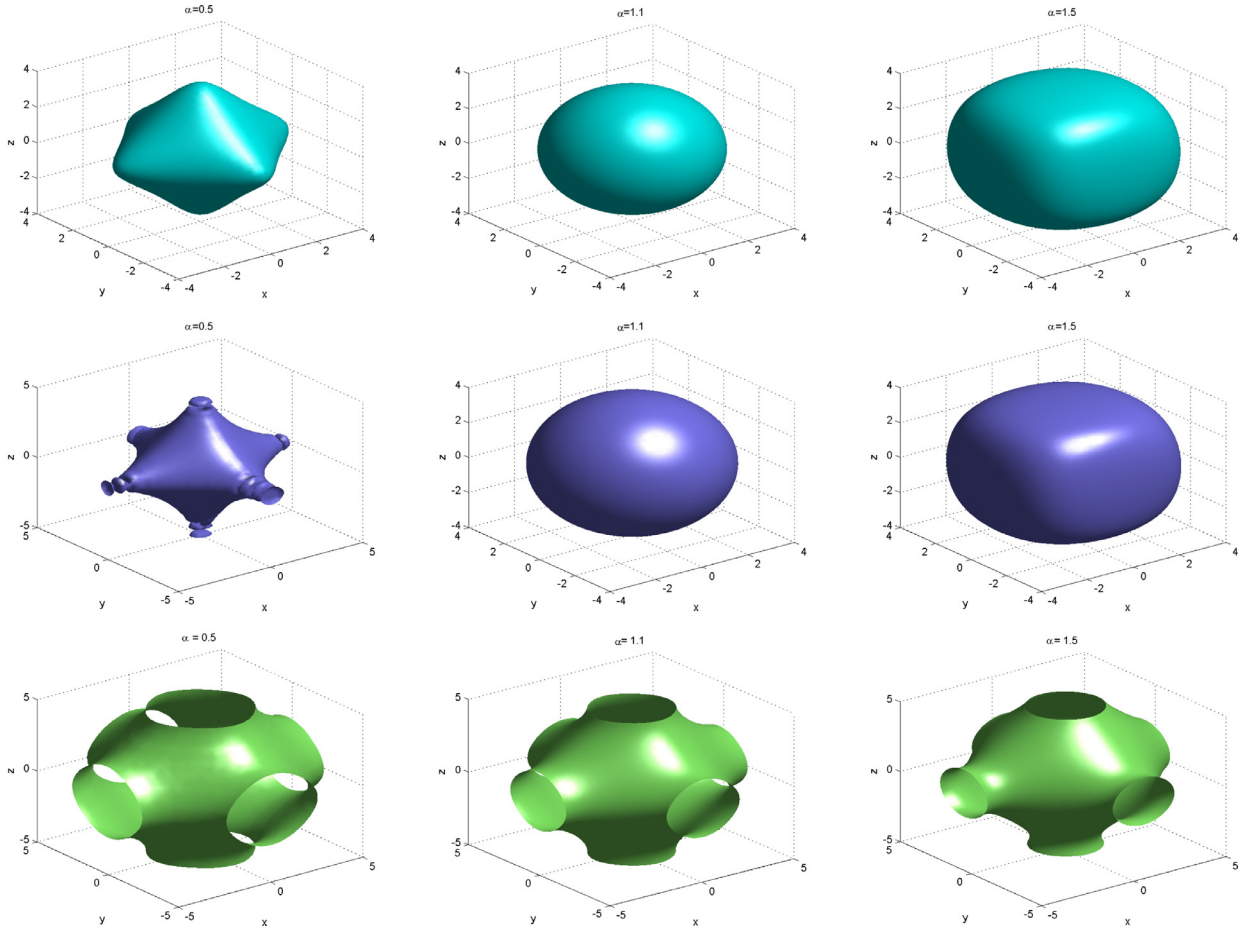


Fig. 4. Simulations in 3D for the fractional activator-inhibitor system (27) at different instants of fractional power α and time t . The first and second rows are obtained for $t = 1$ for U and V respectively. The third row is represents the evolution of species U only at $t = 5$. The first-, second- and third-columns correspond to $\alpha = 0.5$, $\alpha = 1.1$, $\alpha = 1.5$ respectively. Other parameters are $v = 1.0$, $a_0 = -0.1$, $a_1 = 2.0$, $\delta = 4.0$ and $\epsilon = 0.05$.

of chemical species U and V are similar, as a result, we only show for one distribution (for instance, in this example, we report the evolution of U) showing in red and that of V in blue with colour code computed as *shading('interp')*. Also, as seen from Fig. 3, the evolution is nontrivial and the edges of the concentrations (shown the emergence of labyrinthine patterns) are steep and sharp. The set of parameters chosen are

$$\{a_0 = -0.1, a_1 = 2, \delta = 3.8, \epsilon = 0.05, U^* = 0.85, V^* = 0.48\}$$

Further, we simulate the fractional activator-inhibitor system (27) in 3D, subject to initial condition

$$\left. \begin{aligned} U(x, y, z, 0) &= 1 - \exp(-10(x - v/2)^2 + (y - v)^2 + (z - v/2)^2), \\ V(x, y, z, 0) &= \exp(-10(x - v/2)^2 + 2(y - v)^2 + (z - v/2)^2) \end{aligned} \right\} \quad (29)$$

The computational experiment utilizes $128 \times 128 \times 128$ Fourier nodes on a $5 \times 5 \times 5$ grid. In the first and second rows of Fig. 4, we present different dynamics for the evolution of species U and V at different instances of α for $t = 1$. The patterns here changes with $\alpha = 0.5, 1.1, 1.5$ from star-like structure to oval and dice-like shapes. But as simulation time is increasing, the distributions of species the are found to be of the same type for this particular experiment in 3D. Hence we report the distribution of U only in row 3. Results presented in third row at $t = 5$ for $\alpha = 0.5, \alpha = 1.1, \alpha = 1.5$ correspond to the columns 1-3 respectively is a proof to our assertion. It should be noted that evolution of stable patterns possible for the species, for instance in the regime scenario $\alpha \in [1.3, 1.95]$. The evolution of species in the subdiffusive region ($0 < \alpha < 1$) are obviously different, see Fig. 4 for clarity. It should be mentioned that other spatiotemporal dynamics can be obtained depending on the choice of domain size, initial functions and parameter values. The evolution of 3D results reported here can be useful to both artists and fabric pattern designers in pattern generation.

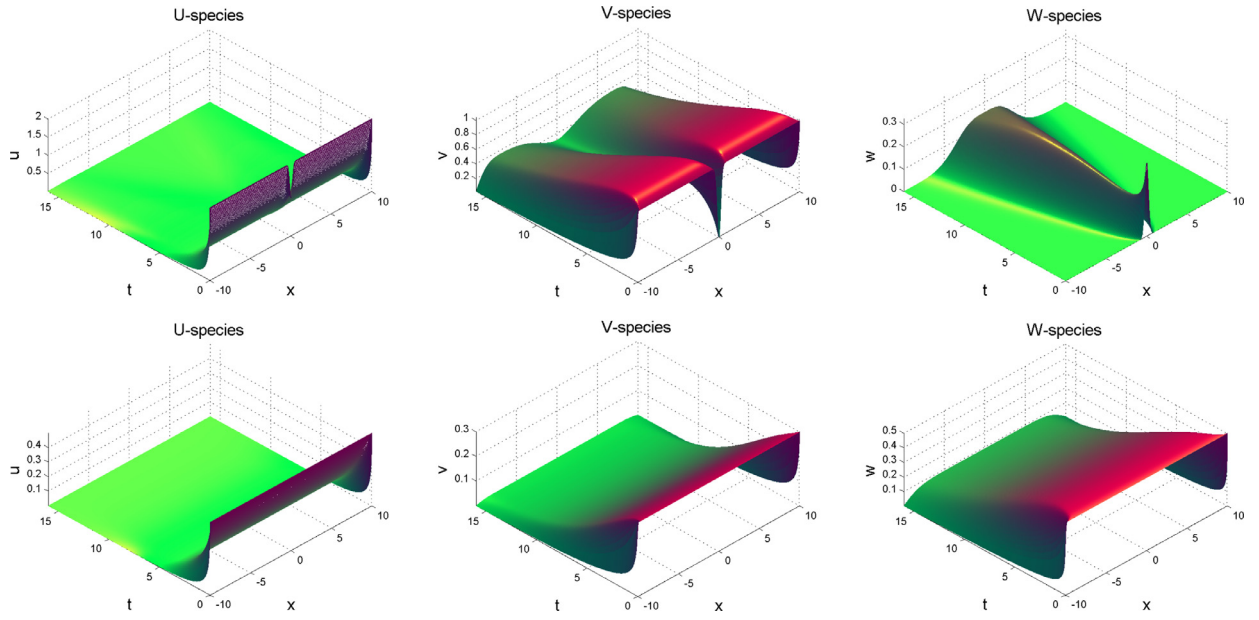


Fig. 5. Surface grey plots of Eq. (30) showing oscillations of the species in phase at different instants of $\alpha = 0.5$ for upper-row and $\alpha = 1.5$ for the lower-row. Parameter values are: $\tau = 0.9$, $\gamma_1 = 0.4$, $\gamma_2 = 0.2$, $\gamma_3 = 0.4$, $\varrho_1 = 0.35$, $\varrho_2 = 0.25$, $\varrho_3 = 0.14$, $\delta_2 = 0.1$, $\delta_3 = 0.1$ and $\zeta_1 = 0.07$, $\zeta_2 = 0.08$, $\zeta_3 = 0.01$.

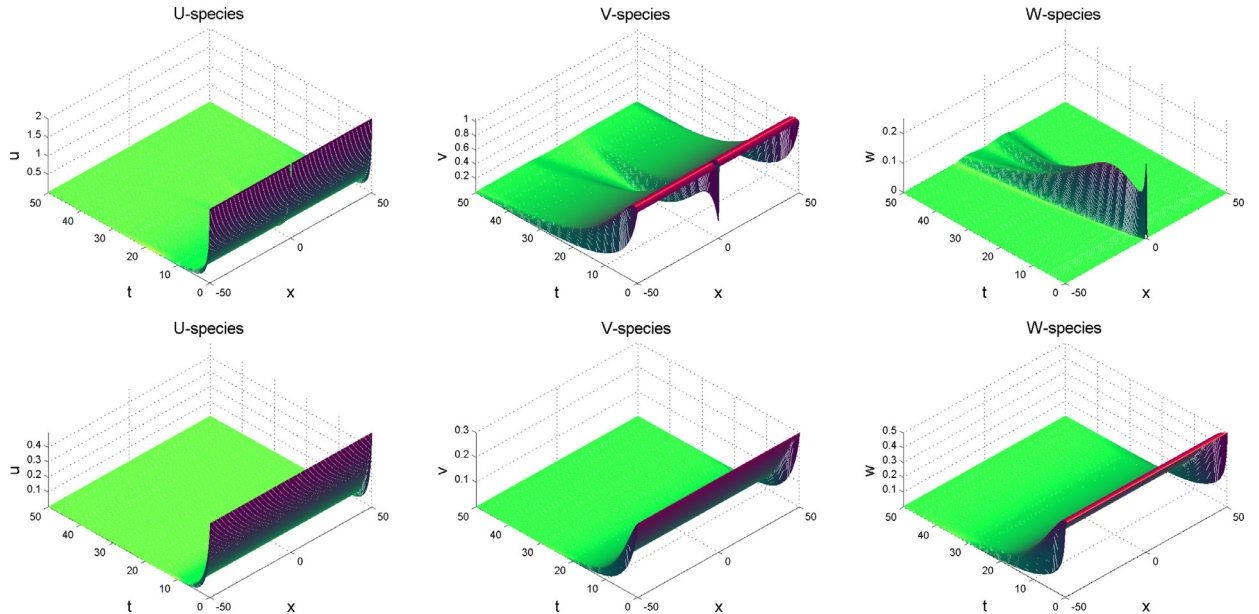


Fig. 6. Spatial evolution system (30) showing the coexistence of the species at final time $t = 50$ for two instances of α with $L = 50$. The upper and lower rows correspond to $\alpha = 0.8$ and $\alpha = 1.75$ respectively. Other parameters are fixed in Fig. 5.

4.3. Three-components example

Predator-prey system: In this section, we extend our numerical experiments to three-components fractional reaction-diffusion systems that describe a complex food chain among the prey u , the predator V and the super-predator w . The equation governing the formulation of ratio-dependent fractional in space predator-prey system with Michaelis-Menten

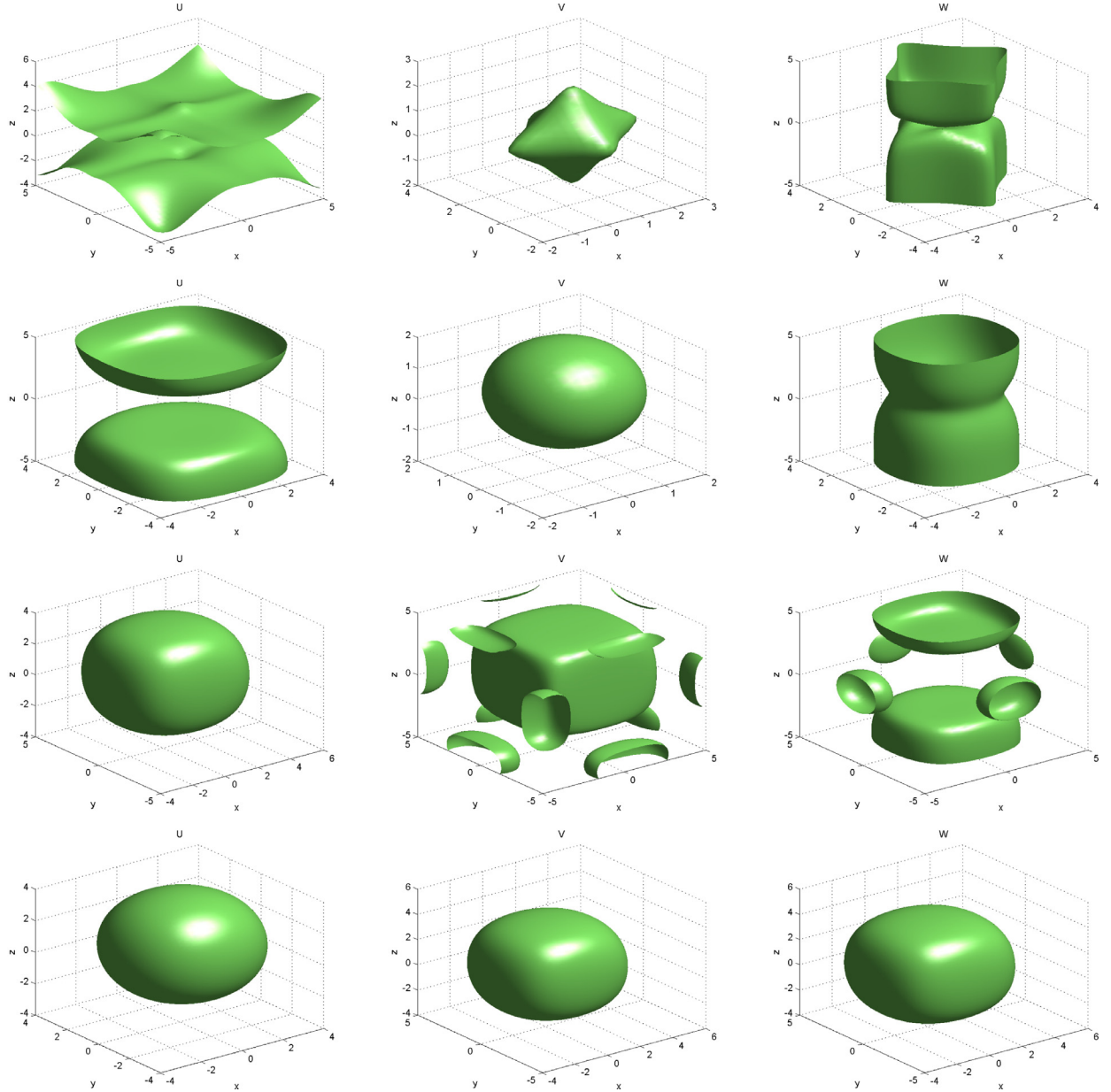


Fig. 7. 3D patterns for the fractional predator-prey Eq. (30) showing the effects of fractional power at different instances of $\alpha = 0.5$ and $\alpha = 1.5$ for respective rows 1 and 2 at final time $t = 10$, $\zeta_1 = 2$, $\zeta_2 = 0.05$, $\zeta_3 = 0.1$ and $p = 1$. Rows 4 and 5 are obtained for $t = 20$ and $t = 40$ at $\alpha = 1.5$. Other parameters are as in Fig. 5.

functional response type [20] is given by

$$\left. \begin{aligned} \frac{\partial u}{\partial t} - \zeta_1 \Delta^\alpha u &= u(\tau - u) - \frac{\gamma_1 uv}{u + v} - \frac{\gamma_2 uw}{u + w}, \\ \frac{\partial v}{\partial t} - \zeta_2 \Delta^\alpha v &= \frac{\varrho_1 uv}{u + v} - \delta_2 v - \frac{\gamma_3 vw}{v + w}, \\ \frac{\partial w}{\partial t} - \zeta_3 \Delta^\alpha w &= \frac{\varrho_2 uw}{u + w} + \frac{\varrho_3 vw}{v + w} - \delta_3 w, \\ \frac{\partial u}{\partial v} = \frac{\partial v}{\partial v} = \frac{\partial w}{\partial v} &= 0 \text{ on } \partial\Omega \times (0, \infty) \\ u(\mathbf{x}, 0) = u_0(\mathbf{x}), v(\mathbf{x}, 0) = v_0(\mathbf{x}), w(\mathbf{x}, 0) = w_0(\mathbf{x}), (\mathbf{x}, t) &\in \Omega \times (0, \infty). \end{aligned} \right\} \quad (30)$$

We simulate (30) in one-dimension, as shown in Fig. 5 at some instances of fractional power α and final time t . It was observed that the species, though coexist but oscillate in phase more in the regime $0 < \alpha < 1$ than in the superdiffusive scenario when $\alpha = 1.5$. The behaviour of species u (prey) and v (predator) are very close and quite different from that of species w (super-predator) that feed on both. This assertion becomes reality and clearly seen on a wide spatial domain, say [-150 150] with $t \geq 60$. The experiment is performed with the initial conditions computed as

$$\left. \begin{array}{l} u(x, 0) = 2 - \exp(-20x^2), \\ v(x, 0) = 1 - \exp(-10x^2), \\ w(x, 0) = \frac{1}{3} \exp(-10x^2), \end{array} \right\} \quad (31)$$

subject to the boundary condition clamped at the end of domain size $\pm L$. To give room for the waves to propagate, we choose a large domain size of $L = 10$ for the experiments.

We experiment numerical results in Fig. 6 with a large domain size of $L = 50$ and final time $t = 50$. We discovered that the distribution of species in the fractional regime $1 < \alpha < 2$ coexist and permanent with increasing time. In the context of biology, this result is useful. It indicates that species can co-habit together in a particular domain for many years without going into extinction.

For the 3D simulations, we compute with the initial conditions

$$\left. \begin{array}{l} u(x, y, z, 0) = 1 - \exp(-10(x - p/2)^2 + (y - p/2)^2 + (z - p/2)^2), \\ v(x, y, z, 0) = \exp(-10(x - p/2)^2 + 2(y - p/2)^2 + (z - p/2)^2), \\ w(x, y, z, 0) = 0.5 - \exp(-10(x - p/2)^2 + (y - p/2)^2 + (z - p/2)^2) \end{array} \right\} \quad (32)$$

to observe different dynamics ranging from irregular to regular (pattern) objects shapes such as oval or egg-like, dice, diamond-like, ring and many others in the regime of fractional order α at instances of $\alpha = 0.5$ and $\alpha = 1.5$, see Fig. 7. The evolution of regular pattern is obtained when the simulation time is increased, we experiment this with $\alpha = 1.5$ as displayed rows 4 and 5 for $t_{max} = 20$ and $t_{max} = 40$ respectively. It should be noted that other dynamical structures (regular or irregular) are possible depending on the choices of initial data and parameter values. The computer simulation results presented in higher dimensions have further provide an evidence that pattern formation in the fractional scenarios, is almost the same as in the standard reaction-diffusion case [16].

5. Conclusion

In this paper, the Fourier spectral method has been introduced as an efficient and viable alternative approach to low order schemes when applied to solve fractional-in-space reaction-diffusion equations. The main merit of this approach is that it results to a full diagonal representation of the fractional operator, and it has the ability to provide spectral convergence regardless of the value of fractional power index α . Some existing reaction-diffusion equations in fractional form are also formulated. In the numerical experiments, a range of illustrative examples in one-, two-, and three-components that are still of current and recurring interest in physics, chemistry and biology in 1D, 2D and 3D which also cover pitfalls and natural questions that may naturally arise is considered. The computer simulation results presented in higher dimensions have further provided an evidence that pattern formation in the fractional scenarios, is almost the same as in the standard reaction-diffusion case. The method presented in this paper is elegant, efficient and reliable for simulating systems of fractional reaction-diffusion problems in higher dimensions. As such, it should be of interest to a broad readership and those interested scholars in the study of nonlinear waves phenomena.

References

- [1] Al-Mohy AH, Higham NJ. Computing the action of the matrix exponential, with an application to exponential integrators. *SIAM J Sci Comput* 2011;33:488–511.
- [2] Aranson IS, Kramer L. The world of the complex Ginzburg–Landau equation. *Rev Mod Phys* 2002;74(99).
- [3] Baeumer B, Kovacs M, Meerschaert MM. Numerical solutions for fractional reaction-diffusion equations. *Comput Math Appl* 2008;55:2212–26.
- [4] Bakkyaraj T, Sahadevan R. Invariant analysis of nonlinear fractional ordinary differential equations with Riemann–liouville fractional derivative. *Nonlinear Dyn* 2015;80:447–55.
- [5] Baleanu D, Masliah SI. Lagrangian formulation of classical fields within Riemann–Liouville fractional derivatives. *Physica Scripta* 2005;70:119–21.
- [6] Berard F, Vandamme CJ, Mancas SC. Two-dimensional structures in the quicic Ginzburg–Landau equation. *Nonlinear Dyn* 2015;81:1413–33. doi:[10.1007/s11071-015-2077-2](https://doi.org/10.1007/s11071-015-2077-2).
- [7] Bhardwaj SB, Singh R, Sharma K, Mishra S. Periodic and solitary wave solutions of cubicquintic nonlinear reaction-diffusion equation with variable convection coefficients. *Pramana-J Phys* 2016;1–6. doi:[10.1007/s12043-015-1177-3](https://doi.org/10.1007/s12043-015-1177-3).
- [8] Botchev MA, Grimm V, Hochbruck M. Residual, restarting and richardson iteration for the matrix exponential. *SIAM J Sci Comput* 2013;35:A1376–97.
- [9] Bueno-Orovio A, Kay D, Burrage K. Fourier spectral methods for fractional-in-space reaction-diffusion equations. *BIT NumerMath* 2014;54:937–54.
- [10] Caputo M. Linear models of dissipation whose Q is almost frequency independent: part II. *J R AstrSoc* 1967;13:529–39. Reprinted in: *Fractional Calculus and Applied Analysis*, 11 (2008) 3–14
- [11] Cartes C, Cisternas J, Descalzi O, Brand HR. Model of a two-dimensional extended chaotic system: evidence of diffusing dissipative solitons. *Phys Rev Lett* 2012;109:178303.
- [12] Chen W, Ye L, Sun H. Fractional diffusion equations by kansa method. *Comput Math Appl* 2010;59:1614–20.
- [13] Cox SM, Matthews PC. Exponential time differencing for stiff systems. *J Comput Phys* 2002;176:430–55.
- [14] Du Q, Zhu W. Analysis and applications of the exponential time differencing schemes and their contour integration modifications. *BIT Numer Math* 2005;45:307–28.

- [15] Gafiychuk V, Datsko B. Pattern formation in a fractional reaction-diffusion systems. *Physica A* 2006;365:300–6.
- [16] Gafiychuk V, Datsko B, Meleshko V. Mathematical modeling of time fractional reaction-diffusion systems. *J Comput Appl Math* 2008;220:215–25.
- [17] Garg M, Manohar P. Numerical solution of fractional diffusion-wave equation with two space variables by matrix method. *Fractional Calculus Appl Anal* 2010;13:191–207.
- [18] Hagberg A, Meron E. From labyrinthine patterns to spiral turbulence. *Phys Rev Lett* 1994;72:2494–7.
- [19] Hanert E. A Comparison of three eulerian numerical methods for fractional-order transport models. *Environ Fluid Mech* 2010;10:7–20.
- [20] Haque M. Ratio-dependent predator-prey models of interacting populations. *Bull Math Biol* 2009;71:430–52.
- [21] Hassan IH. Comparison differential transform technique with adomian decomposition method for linear and nonlinear initial value problems. *Chaos, Solitons Fractals* 2008;36:53–65.
- [22] Henry BI, Langlands TA, Wearne SL. Turing pattern formation in fractional activator-inhibitor systems. *Phys Rev E* 2005;72:026101.
- [23] Hu L, Chen D, Wei GW. High-order fractional partial differential equation transform for molecular surface construction. *Mol Based Math Biol* 2013;1:1–25.
- [24] Kassam AK, Trefethen LN. Fourth-order time stepping for stiff PDEs. *SIAM J Sci Comput* 2005;26:1214–33.
- [25] Khader MM. On the numerical solutions for the fractional diffusion equation. *Commun Nonlinear Sci Numer Simulat* 2010;16:2535–42.
- [26] Kilbas AA, Luchko YuF, Martnez H, Trujillo JJ. Fractional fourier transform in the framework of fractional calculus operators. *Integral Transforms Special Functions* 2010;21:779–95.
- [27] Kilbas AA, Srivastava HM, Trujillo JJ. Theory and applications of fractional differential equations. Elsevier, Netherlands; 2006.
- [28] Li X, Xu C, Li X, Xu C. A Space-time spectral method for the time fractional diffusion equation. *SIAM J Numer Anal* 2009;47:2108–31.
- [29] Li X, Xu C. Existence and uniqueness of the weak solution of the spacetime fractional diffusion equation and a spectral method approximation. *Commun Comput Phys* 2010;8:1016–51.
- [30] Liu Q, Liu F, Gu Y, Zhang P, Chen J, Turner I. A Meshless method based on point interpolation method (PIM) for the space fractional diffusion equation. *Appl Math Comput* 2015;256:930–8.
- [31] Luan VT, Ostermann A. Explicit exponential Runge–Kutta methods of high order for parabolic problems. *J Comput Appl Math* 2014;256:168–79.
- [32] Lubich C. Discretized fractional calculus. *SIAM J Math Anal* 1986;17:704–19.
- [33] Luchko Y, Gorenflo R. An operational method for solving fractional differential equations with the caputo derivatives. *Acta Math Vietnamica* 1999;24:207–33.
- [34] Miller KS, Ross B. An introduction to the fractional calculus and fractional differential equations. Wiley, New York; 1993.
- [35] Mohyud-Din ST, Noor MA. Variational iteration method for solving higher-order nonlinear boundary value problems using he's polynomials. *Int J Nonlinear Sci Numer Simulat* 2008;9: 141–57.
- [36] Momani S, Odibat Z. Variation iteration method for solving the space-and time-fractional KdV equation. *Numer Methods Partial Differ Equ* 2007b;24:262–71.
- [37] Momani S, Odibat Z, Erturk VS. Generalized differential transform method for solving a space and time-fractional diffusion-wave equation. *Phys Lett A* 2007;370:379–87.
- [38] Momani S, Odibat Z. A Novel method for nonlinear fractional partial differential equations: Combination of DTM and generalized taylor's formula. *J Comput Appl Math* 2008;220:85–95.
- [39] Odibat Z, Momani S. Application of the variation iteration method to nonlinear differential equations of fractional order. *Int J Nonlinear Sci Numer Simul* 2006;7:15–27.
- [40] Odibat Z, Shawagfeh N. Generalized Taylor's formula. *Appl Math Comput* 2007;186:286–93.
- [41] Odibat Z, Bertelle C, Aziz-Alaoui MA, Duchamp GH. A Multistep differential transform method and application to non-chaotic or chaotic systems. *ComputMath Appl* 2010;59:1462–72.
- [42] Odibat Z, Momani S. Numerical methods for nonlinear partial differential equations of fractional order. *ApplMathModel* 2008;32:28–39.
- [43] Owolabi KM. Symmetric linear multistep methods for direct solution of second order initial value problems of ordinary differential equations. Federal University of Technology Akure; 2007. M.tech thesis. (Unpublished)
- [44] Owolabi KM, Patidar KC. Higher-order time-stepping methods for time-dependent reaction-diffusion equations arising in biology. *Appl Math Comput* 2014;240:30–50. <http://dx.doi.org/10.1016/j.amc.2014.04.055>
- [45] Owolabi KM. Robust IMEX schemes for solving two-dimensional reaction-diffusion models. *Int J Nonlinear Sci Numer Simul* 2015;16:271–84. doi:10.1515/ijnsns-2015-0004.
- [46] Owolabi KM, Patidar KC. Existence and permanence in a diffusive kiSS model with robust numerical simulations. *Int J Diff Equ* 2015;2015(8):485860. doi:10.1155/2015/485860.
- [47] Owolabi KM, Patidar KC. Numerical simulations of multicomponent ecological models with adaptive methods. *Theor Biol Med Model* 2016a;13. doi:10.1186/s12976-016-0027-4.
- [48] Owolabi KM, Patidar KC. Effect of spatial configuration of an extended nonlinear kiersteadslobodkin reaction transport model with adaptive numerical scheme. Springer Plus 2016b;5:303. doi:10.1186/s40064-016-1941-y.
- [49] Paradis E, Baillie SR, Sutherland WJ. Modeling large-scale dispersal distances. *Ecol Model* 2002;151:279–92.
- [50] Podlubny I. Fractional differential equations. Academic Press, New York; 1999.
- [51] Podlubny I, Chechkin A, Skovranek T, Chen YQ, Jara BB. Matrix approach to discrete fractional calculus II: partial fractional differential equations. *J Comput Phys* 2009;228:3137–53.
- [52] Ray SS. Analytical solution for the space fractional diffusion equation by two-step Adomian Decomposition method. *Commun Nonlinear Sci Numer simul* 2009;14:1295–306.
- [53] Yu Q, Liu F, Turner I, Burrage K. Stability and convergence of an implicit numerical method for the space and time fractional Bloch-Torrey equation. *Philos Trans R Soc A* 371:20120150. (doi.org/10.1098/rsta.2012.0150).
- [54] Sabatier J, Agrawal OP, Machado JAT. Advances in fractional calculus: Theoretical developments and Applications in physics and Engineering. Springer, Netherlands; 2007.
- [55] Samko SG, Kilbas AA, Marichev OI. Fractional integrals and derivatives: theory and applications. Gordon and Breach, Amsterdam; 1993.
- [56] Samko S. Denseness of the spaces ϕ_Y of Lizorkin type in the mixed $L_p(r_n)$ -spaces. *Studia Mathematica* 1995;113:199–210.
- [57] Sousan E, Li C. A Weighted finite difference method for the fractional diffusion equation based on the riemann-liouville derivative. *Appl Numer Math* 2015;90:22–37.
- [58] Theocaris G, Frantzeskakis DJ, Kevrekidis PG, Malomed BA, Kivshar Y. Ring dark solitons and vortex necklaces in Bose–Einstein condensates. *Phys Rev Lett* 2003;90:120403.
- [59] Tokman M. A New class of exponential propagation iterative methods of Runge–Kutta type (EPIRK). *J Comput Phys* 2011;230:8762–78.
- [60] Tokman M, Loffeld J, Tranquilli P. New adaptive exponential propagation iterative methods of runge-kutta type. *SIAM J Sci Comput* 2012;34:A2650–69.
- [61] Wang H, Du N. A Super fast-preconditioned iterative method for steady-state space fractional diffusion equations. *J Comput Phys* 2013;240:49–57.
- [62] Yildirim A, Mohyud-Din ST. Analytical approach to space and time fractional Burger's equation. *Chin Phys Lett* 2010a;27:090501.
- [63] Yildirim A, Mohyud-Din ST. The numerical solution of the three-dimensional Helmholtz equations. *Chin Phys Lett* 2010b;27:060201.
- [64] Yu Q, Liu F, Anh V, Turner I. Solving linear and non-linear space fractional reaction-diffusion equations by the adomian decomposition method. *Int J Numer Methods Eng* 2008;74:138–58.
- [65] Zeng F, Li C, Liu F, Turner I. Numerical algorithms for time-fractional subdiffusion equation with second-order accuracy. *SIAM J Sci Comput* 2015;37:A55–78.

- [66] Zeng F, Liu F, Li C, Burrage K, Turner I, Anh V. A Crank-nicolson ADI spectral method for a two-dimensional riesz space fractional nonlinear reaction-diffusion equation. SIAM J Numer Anal 2014;52:2599–622.
- [67] Zheng M, Liu F, Turner I, Anh V. A Novel high order space-time spectral method for the time fractional fokker-planck equation. SIAM J Sci Comput 2015;37:A701–24.
- [68] Zhou Y. Basic theory of fractional differential equations. World Scientific, New Jersey; 2014.